Proceedings of ASME Turbo Expo 2003
Power for Land, Sea, and Air
June 16-19, 2003, Atlanta, Georgia, USA

GT-2003-38638

ABILITY OF A POPULAR TURBULENCE MODEL TO CAPTURE CURVATURE EFFECTS: A FILM COOLING TEST CASE

Satish Undapalli and James H. Leylek
Advanced Computational Research Laboratory
Department of Mechanical Engineering
Clemson University
Clemson, SC 29634

ABSTRACT

Computations are performed in conjunction with code validation quality experiments found in the open literature to specifically address the usage of popular two-equation eddy viscosity models in day-to-day gas turbine applications. In such simulations many features such as pressure gradients, curvature effects are present. The present work is focused on testing a popular turbulence model to resolve film cooling on curved surfaces. A systematic computational methodology has been employed in order to minimize numerical errors and evaluate the performance of a popular turbulence model. The test cases were examined for a single row of holes, blowing rates ranging from 1 to 2.5, isolated effects of convex and concave curvature on film cooling, density ratio close to 2, and an injection angle of 35°. Key aspects of the study include: (1) extremely dense, high quality, multi-block, multi-topology grid involving over 3 million finite volumes; (2) higher order discretization; (3) turbulence model with two-layer near-wall treatment; (4) strict convergence criteria; and (5) grid independence. A fully-implicit, pressure-correction Navier-Stokes solver is used to obtain all the solutions. Results for adiabatic cooling effectiveness are compared with measurements in order to document the: (1) Range of applicability of the present modeling capability; and (2) Possible reasons for discrepancies. The data shows that the computations predicted the effects of curvature on mean flow, however effect on turbulence field is not captured. A clear set of recommendations is provided for future treatments of this class of problems.

Keywords: CFD, Convex, Concave, Curvature, RANS, Turbulence Modeling

NOMENCLATURE

D	film-cooling hole diameter [m]
DNS	Direct Numerical Simulation
DR	coolant-to-mainstream density ratio = ρ_j/ρ_∞
I	coolant-to-mainstream momentum flux ratio $=\rho_j U_j^2/\rho_\infty U_\infty^2$
k	turbulent kinetic energy [m^2/s^2]
L	film hole length [m]
LES	Large Eddy Simulation
M	coolant to mainstream mass flux ratio = $\rho_j U_j/\rho_\infty U_\infty$
Ma	Mach number
MF	coolant mass fraction
Re	Reynolds number
RANS	Reynolds Averaged Navier Stokes
RKE	Realizable k-ε turbulence model
r	radius of curvature [m]
2r/D	strength of curvature parameter
x	streamwise coordinate originating at trailing edge of film holes [m]
y	coordinate normal to test surface [m]
y^+	non-dimensional wall distance
z	spanwise coordinate originating at film hole centerline [m]
δ	boundary layer thickness at injection [m]
ε	dissipation rate of turbulent kinetic energy [m^2/s^3]
η	impermeable wall effectiveness $= (MF_w - MF_\infty)/(MF_j - MF_\infty)$
$\overline{\eta}$	laterally averaged impermeable effectiveness
ρ	density [kg/m^3]

Subscripts

∞	mainstream conditions at crossflow inlet plane
j	coolant jet conditions
w	local wall value

1. INTRODUCTION

Film cooling is often used to protect gas turbine airfoils from exposure to hot combustor gases. It involves injecting a coolant gas, usually bled from the aft stages of the high-pressure compressor, through holes in the surfaces of the hollow turbine airfoils. This coolant spreads along the airfoil's outer surfaces, protecting it from the hot mainstream. Because modern day gas turbine engines run with high turbine inlet temperatures to reach higher efficiencies, film cooling has become a critical technology for turbine design. Consequently, there is an urgent need to study the physical processes

in film-cooling flows, and to develop predictive capability to be used in the design process.

Film cooling has been studied extensively for the past 30 years. Most of these studies can be divided into two main categories. The first includes experiments on specific airfoil geometries that are conducted close to engine conditions. These studies, though very important to determine the film cooling performance at the design conditions, often do not deliver enough information to study the off-design conditions and different geometries. The second category includes experiments that isolate the different features of the flow over an airfoil. Some of the features investigated include the effects on film cooling of:

- Favorable and adverse pressure gradients
- Curvature effects (convex and concave)
- Free stream turbulence
- Boundary layer thickness

The above fundamental studies are critical to understanding the overall physics of film cooling flows. These experiments are also useful as validation cases for studying computational approaches to film-cooling prediction, since any computational technique depends on the ability to correctly resolve the physical mechanisms in film-cooling flows.

The open literature does not provide any comprehensive numerical study of the influence of curvature on film cooling. Design of the critical cooling technology is currently based on empirical correlations. The gas turbine industry could greatly benefit from a predictive, numerical design tool. Hence there is a need for truly predictive capability based on relatively simple, robust, economical CFD based design tools. This could lead to a significant reduction in the overall design cycle time.

The ability of CFD to capture the curvature effects is critically important in many gas turbine applications. Turbine aerodynamics and heat transfer applications primarily use two-equation eddy viscosity models. The present work, although focuses on film cooling, evaluates the performance of a popular turbulence model such as realizable k-ε (RKE). Simulations are conducted to compute the adiabatic film-cooling effectiveness on convex and concave surfaces and compare the results with experiments available in the open literature. These simulations show where CFD stands regarding curvature effects in film cooling.

2. LITERATURE REVIEW

2.1 Experimental Studies

The effects of curvature on airfoil film cooling can be understood only if the streamline curvature effects on turbulent flow are understood. Numerous experiments can be found in the literature investigating these effects. These studies show that streamline curvature produces significant changes in the turbulent structure of shear layers. These changes are usually an order of magnitude more important than normal pressure gradients and other explicit terms appearing in the mean motion equations of shear layers. This was first stated by Bradshaw [1] in his report on the effects of streamline curvature on turbulent flow. So and Mellor [2] confirmed that curvature has a substantial effect on the nature of the mean flow and Reynolds stresses and, consequently, the wall shear stress. Muck et al. [3,4] conducted experiments to determine the effect of turbulence on boundary-layer development on convex and concave surfaces. They concluded that convex curvature has a stabilizing effect and concave curvature has a destabilizing effect in the boundary layer and that these effects are fundamentally different from one another. They found that even mild convex curvatures tend to attenuate the turbulence, while concave curvature results in quasi-inviscid generation of longitudinal vortices, together with significant enhancement in turbulence caused by both the curvature and the vortices. These vortices are called Taylor-Görtler vortices and have been observed in most experiments conducted on boundary layers on concave surfaces.

Ito et al. [5] measured local film cooling effectiveness on turbine airfoil geometry using a mass transfer technique. They explained the influence of curvature on film-cooling effectiveness by considering the balance of forces exerted on the fluid of the jet by the static pressure and centrifugal force along the path of the coolant. They determined that curvature influences the mean flow independent of the Reynolds stresses, by forcing coolant jets toward a convex surface at low momentum-flux ratios (I) and away from the wall at higher I. The trend was reversed on concave surfaces. Goldstein et al. [6] studied the importance of curvature on film cooling on both the pressure (concave) and suction (convex) sides of a turbine blade. The authors used two rows of staggered holes in their experiments and found that at low and moderate blowing rates the effectiveness is better on a convex than on a concave surface. At high blowing rates the effectiveness was not greatly influenced by the surface curvature. The influence of curvature, however, was much less than was found with injection through a single row of holes where the individual jets tend to act more independently. Makino and Kumado [7] performed many film cooling experiments to study the curvature effects. All the experiments were performed for a small range of blowing ratios and the momentum flux ratios less than unity.

Schwarz and co-workers [8-10] performed experiments on film cooling in curved passages. The studies focused on the influence of strength of curvature -- expressed by the parameter 2r/D -- on the impermeable wall effectiveness. The effects of curvature were isolated by fixing both the radius of curvature and the boundary-layer displacement thickness at the point of injection for all the cases considered. Similar to Ito et al. [5], the authors concluded that the tangential momentum of jets reduces effectiveness on the convex surface, and improves it on the concave. The radius of curvature of the jet trajectory is increased as tangential momentum is increased, pulling it away from a convex wall and pushing it into a concave wall. The normal momentum of jets degrades effectiveness on all surfaces by lifting the jet away from the wall in the near field. As a consequence, the convex surface shows better cooling performance than the concave at low momentum flux ratio, and the reverse is true for higher I values. Lateral profiles of local effectiveness are much flatter on the concave surface than on the convex, and this is attributed to lateral mixing caused by the unstable concave flow. Beyond a momentum flux ratio of 2, however, changes in curvature appeared to have little effect on cooling performance.

Recently, film-cooling experiments on convex surfaces were conducted by Lutum et al. [11]. The adiabatic film-cooling effectiveness and heat transfer increase due to film injection was investigated for a convex surface with zero streamwise pressure gradients. The effect of convex curvature was to decrease film-cooling effectiveness and increase heat transfer coefficient at moderate and high blowing rates.

2.2 Numerical Studies

Several numerical studies have been performed for film cooling on flat plates. Walters and Leylek [12] documented a systematic computational methodology for this class of problems, in which turbulence model performance is isolated by minimizing errors arising from either inaccurate computational model or numerical viscosity.

Very few numerical studies on curvature effects are available in the open literature. One exception is the study of Berhe and Patankar [13,14], which compared computational simulations with selected experiments of Schwarz [8]. They modified the k-ε turbulence model to account for the curvature effects on the Reynolds stresses and turbulent heat fluxes. The results showed reasonable agreement with measured data. The simulations only considered relatively low trajectory jets, corresponding to blowing ratios equal to 0.5 and 1.0, and momentum flux ratios of 0.125 and 0.5, respectively. This does not allow an accurate judgment regarding model performance in cases with coolant jet lift-off. However, for the cases with attached coolant jets, the curvature-modified turbulence model appeared to yield some improvement over unmodified models.

Lin and Shih [15] performed computational studies comparing flat and convex surfaces. They used a low Reynolds number k-ω/SST turbulence model that was not modified to account for curvature effects on turbulence. The curved geometry was similar to the one used by Schwarz [8]. One significant departure of the computational model from the experiments was the use of a plug flow inlet boundary condition. The experiments had maintained the velocity profile at the injection location to yield a constant δ/D for each of the test cases. The results were only compared to experimental data for the case of flat-plate injection at the lowest blowing ratio (M = 0.5), so an accurate assessment of the predictive capability was not possible for either curvature effects or significant jet lift-off.

2.3 Summary

Almost every study on curvature effects concludes that little progress has been made in quantifying the effects of curvature on turbulence despite the level of effort devoted to the subject through laboratory experiments, modeling and computational study. Some aspects are clear, however. Most specifically the conclusion that convex curvature tends to suppress boundary-layer turbulence and that concave curvature tends to augment it.

Experimental studies of film cooling on curved surfaces have demonstrated two important yet separate effects: the influence of curvature on the mean flow characteristics (e.g. Ito et al., [5]), and the influence of curvature on the Reynolds stress and turbulent heat flux (e.g. Mayle et al., [16]). From a computational standpoint, one would expect current simulation techniques to resolve the former with at least reasonable accuracy, but resolving the latter depends greatly on the turbulence treatment used in the computations.

There are very few computational studies on film cooling of a curved surface and unfortunately these studies do not eliminate all the usual sources of errors in CFD simulations. The present study addresses computational issues such as proper modeling, geometry, grid density and quality, discretization schemes, convergence and grid independence. The errors due to these issues are made negligible in order to provide a better understanding of the performance of turbulence models in simulations of film cooling on curved surfaces. Results are presented and compared to experimental data for a much wider range of conditions than has been found in the literature to date. This includes a range of blowing and momentum flux ratios to cover attached and highly lifted coolant jets, as well as examination of different strengths of curvature on convex and concave sides. Results will be examined in order to yield an evaluation of current modeling techniques, and to make suggestions for future improvements to the predictive capability of Computational Fluid Dynamics.

3. COMPUTATIONAL METHODOLOGY

3.1 Validation experiments

The present simulations are compared to the experiments of Schwarz [8]. The experimental apparatus, shown in Figure 1, consists of five major components: wind tunnel, test section, secondary injection system, sampling system, and data acquisition/reduction system. The convex working surface has a radius of curvature of 10.10 cm and is 135° long in the streamwise direction. Stainless steel tubes of required film hole diameter are epoxied into the holes drilled through the curved surfaces at an angle of 35° in the streamwise direction. The centers of the injection holes are located at 45° after the onset of convex curvature and at 42.5° after the onset of concave curvature. The aspect ratio of the test section used in the experimental set up is 4.79. Effectiveness measurements along both the convex and concave wall of the test section are made using a foreign gas injection technique. Air mixed with Freon12 (density ratio = 2) is injected through the row of holes in the curved surfaces. Detailed velocity profiles, and a description of how they were obtained, can be found in Schwarz [8]. The following table shows the test cases considered for the present computational studies.

Table 1: Test cases

	Convex curvature		Concave curvature
Curvature strength (2r/D)	126	61	-58
Blowing rates (M)	1.00, 1.21 1.59, 2.48	1.00, 1.33, 1.90	0.92, 1.30, 2.17

3.2 Computational Model

Figure 2 shows film-hole centerline plane view of the 3-D computational domain for the convex curvature film cooling study. The computational domain for the concave curvature study is similar to Figure 2 with the difference that the film hole and plenum are located on the concave side. It includes three main zones: the curved passage region, the film hole, and the coolant supply plenum. Flow in each of the three zones must be modeled simultaneously for accurate simulation. There is strong coupling between the three regions and a very complex flow structure in the film hole which causes the jet exit conditions to change dramatically with blowing ratio (Walters and Leylek, [12]; Lin and Shih, [15]). For the present simulations, the different non-dimensional curvature strengths (2r/D) are implemented by changing the film-hole diameter, and maintaining the passage curvature for each case, exactly as was done in the experimental study. Unlike most other film-cooling cases, the film holes in the present geometry have a projection into the plenum. The film holes also have a relatively high length-to-diameter ratio (L/D) equal to 10. The flow symmetry requires a model only one-half pitch in the lateral (spanwise) direction. This simplifies the computational model as well as reduces the cell count. Symmetry conditions are applied at both the film-hole centerline plane and the mid-pitch plane between adjacent film holes which models infinite row of jets. This is allowed since the aspect ratio of the test section is large and the sidewalls have no appreciable effect.

It is important to use the appropriate boundary conditions in order to make sure that an accurate analog to the experiments is simulated. For the main passage flow, an inlet velocity profile is used in the current study in order to include any upstream boundary-layer history effects. The authors conducted numerical experiments using a 2-D passage model, in order to obtain the correct form of the inlet profile. The inlet profile was adjusted in such a way that this

profile matched the mass flow rate, Reynolds number reported in the experiments and also showed good agreement with the experimental data provided at the injection location without film cooling. The velocity profile at the injection location is shown in Figure 3 both for the case of uniform inlet flow and for the profile used in this study. Similar exercise is carried out to obtain the profile on the concave side. The corresponding inlet profiles are used for the simulations on the convex and concave sides. The profiles for turbulent kinetic energy and turbulent dissipation rate were also taken from the two dimensional simulations and applied to the film-cooled cases. The above procedure does require extra effort, but was deemed necessary since the boundary-layer thickness to film-hole diameter ratio (δ/D), as well as the boundary layer shape factor (momentum content of the boundary layer), are known to be important parameters in film-cooling performance.

The other boundary conditions are relatively straightforward. A constant pressure was applied at the outlet in order to avoid any recirculation. The plenum is specified as a velocity inlet. Because the plenum "pressurized" during the simulations, resulting in a changed inlet density, an iteration procedure was adopted to exactly match the experimental mass flow rate at the plenum inlet. A secondary coolant gas consisting of air and Freon-12 was introduced at the plenum inlet to match the foreign gas used in the experiments. All the walls were declared adiabatic. All the properties were assumed to follow ideal gas mixture behavior, and Sutherland's law for temperature dependent molecular viscosity was used. The Reynolds number based on the passage freestream velocity and film-hole diameter ranged from 430,000 for the weak curvature case to 890,000 for the strong curvature case on the convex side. On the concave side, the highest curvature considered has a Re of 1892,000 based on the parameters mentioned above. The Mach number at the inlet plane of the crossflow passage was 0.116 for all cases.

3.3 Grid

The computational grid must be constructed to meet several objectives. The grid must completely and accurately resolve the computational domain, avoiding as much as possible either stair-step or faceted boundary definition. The grid should be fine in critical areas of the flowfield and in areas where there are steep gradients of the flow variables. At the same time, grid quality must be maintained, in terms of aspect ratio, stretching ratio, and cell skewness factors. To meet these objectives, the current study implements a grid methodology that is multi-block, multi-topology, unstructured, and adaptive. First, the domain is subdivided into several smaller sub-domains using the so-called "super block" scheme, each of which is meshed using an appropriate topology. Topologies used include hexahedra, tetrahedra, triangular prisms, and pyramids. Typically, triangular prisms or hexahedra are used in boundary layers where cells of large aspect ratio can be grown. Tetrahedral cells are used to fill complex volumes and near walls in regions where flow separation is likely to occur (e.g. film-hole inlet and exit) in order to maintain aspect ratios near unity. Pyramid cells are used for a transition from prisms to tetrahedrons. It is to be noted that the first grid point adjacent to all the bounding wall surfaces is spaced for a y^+ of approximately unity in order to meet the requirements for the two-layer near wall treatment as explained in the turbulence model section below.

Two separate background meshes were generated, one for each strength of curvature investigated on the convex side. On the concave side, one curvature strength is considered and a background mesh was generated for this. The background grids were generated using a combination of the I-DEAS solid modeling package from SDRC, Inc. and the Gambit and T-Grid pre-processing tools from Fluent, Inc. The cell count of the background grid was approximately 3.3 million finite volume cells. Figures 4a and 4b show different views of the background grid, and highlight the use of the multi-block, multi-topology approach. For each simulation, grid independence was obtained by solution-based adaption. Once convergence was obtained on the background grid, the mesh was refined based on gradients of all primary variables, with an increase in mesh size of approximately 20%. The solution was then converged on the new grid and compared to the previous result. The process was repeated until the change in local film-cooling effectiveness on the downstream surface was negligible. For the present simulations, it was found that the background meshes yielded grid independent solutions for all cases.

3.4 Solution Method

The present study uses a second order discretization scheme in order to obtain more accurate resolution of the flow field. In the present work the solver used was Fluent version 5.5.14. Within Fluent, the segregated solver was implemented, which uses an implicit pressure-correction based algorithm (SIMPLE), which is appropriate for the low Ma cases investigated herein. To obtain rapid convergence, the computational domain is initialized with the average values of all the flow parameters. The under-relaxation factors had to be managed in a systematic manner to get convergence. For all cases, the solution was declared converged using the following unusually strict set of four criteria: first, a reduction in normalized residuals of at least three orders of magnitude along with the leveling-off of these quantities; second, a reduction of the global mass imbalance to less than .01% of the plenum mass flow rate; third, monitoring of the local values of velocity magnitude and turbulence quantities (k and ε) at a point located in the critical portion of the computational domain to determine that they were not changing with increasing iteration; and fourth by monitoring the profiles of the above mentioned quantities at a plane location. As described in the above section, solution-based adaption was used to determine grid independence.

The simulations were run on a cluster of Sun Microsystems Ultra 80 computers connected in parallel through a gigabit switch and a fibre optics network with 8 processors and 8 gigabytes of RAM. The lowest blowing ratio was run first, and between 3000 and 4000 iterations were required for convergence. Subsequent blowing rate simulations were started from the previous solution, and convergence was attained after about 2000 iterations.

3.5 Turbulence modeling

The most commonly used turbulence models for film-cooling problems are of the two-equation eddy-viscosity type. The most basic and popular of these is the standard k-ε model. Earlier studies by Walters and Leylek [17] show that this model tends to underpredict the turbulence levels near the film-hole exit and overpredict them farther downstream. It has also been pointed out by several authors (Durbin [18], Moore and Moore [19], Walters and Leylek [20]) that the standard k-ε model suffers from violation of the realizability constraints, and should not be used for problems in which the turbulence is expected to depart strongly from equilibrium. Walters and Leylek [20] examined the impact of film cooling on total pressure loss through a turbine cascade, and concluded that the realizable k-ε model (RKE) (Shih et al. [21]) available in Fluent yielded results similar to a full Reynolds Stress Model and was consequently the best choice of available eddy-viscosity model for this class of problems.

It must be pointed out that the RKE model used in the present study is not modified in order to establish a reference for the eddy-viscosity models. One of the questions this study is designed to answer is how necessary it is to include curvature modifications into this class of modeling, in order to resolve film cooling on curved surfaces. In fact, from the point of view of gas turbine designers involved in either aerodynamic or heat transfer (with or without film cooling), it is helpful to determine the accuracy of current modeling practice before insisting on more complicated models, which may suffer from numerical stiffness and increased computational expense.

In addition to the turbulence model used, the choice of near wall treatment is critical to any RANS simulation. Typically, the viscous sublayer and buffer region are bridged using wall functions, which relate the wall shear stress to the first cell velocity using some form of the law of the wall. In a different wall treatment, the transport equations are integrated to the wall itself, and the viscous and buffer regions are fully resolved. For these sublayer-resolving methods, the high-Re forms of the turbulence models must be modified in some way in order to include the influence of wall proximity on turbulence quantities. Because film cooling involves complex interaction between the coolant jet and the oncoming crossflow, including separation of both the coolant and crossflow boundary layers, it is necessary to implement some type of sublayer-resolving model in order to accurately capture the details of the relevant physical mechanisms. In the present study, the two-layer model of Wolfstein [22] is used for all simulations. This model has been shown to yield favorable results in near-wall flows, even when compared to more complex low-Re two-equation models (Chen and Patel, [23]). This model has also been shown to yield improved near-field results in film-cooling flows when compared to the wall function approach (Walters and Leylek, [17]). Thus there is a need to employ two-layer near-wall treatment in the present study. Care is taken to generate all the grids with $y^+ \leq 1$ for all the wall cells everywhere in the domain to fully resolve the viscous sublayer as required by the two-layer model.

4. COMPARISON OF CFD AND EXPERIMENTAL RESULTS

4.1 Convex Curvature

This section compares the computational results on the convex curvature with the experimental data from Schwarz [8]. The comparison highlights the applicability of the described numerical method to film cooling on convex surfaces. This also highlights the applicability of the realizable k-ε (RKE) model in predicting the turbulent mixing of the exiting coolant, and its impact on film cooling performance.

The results from the low strength-of-curvature case (2r/D = 126) will be examined first. Figure 5 shows the laterally averaged adiabatic wall effectiveness for Freon injection (DR = 2) plotted versus x/D for blowing ratios (M) ranging from 1 to 2.5. These plots are obtained by integrating the local lateral profiles of impermeable wall effectiveness using the trapezoidal rule. For the lowest M, the CFD results show a significant underprediction of the effectiveness in the near field, with improving agreement further downstream. From about x/D = 20 onward, the computations show only a slight underprediction of the experiments. This suggests that the computations are able to predict the downstream mixing with reasonable accuracy. This is likely due to the fact that the coolant remains within the passage boundary layer for this relatively low injection rate. The trends for the two highest M are considerably different. For these cases, the computations indicate a clearly detached coolant jet. However, the computations show a very rapid rise in effectiveness corresponding to the transport of the coolant back toward the downstream surface, while the experiments show a very slow rise.

Figure 6 shows streamwise variation of local impermeable effectiveness values for two bounding cases, M = 1 (a) and M = 2.5 (b), at different spanwise locations corresponding to z/D = 0 (centerline) and z/D = 0.732. Again these results are for the low strength of curvature. The centerline effectiveness (z/D = 0) is directly tied to the jet lift-off. For the lower M case, where I is low, the centerline effectiveness is well predicted, while the off-centerline (z/D = 0.732) values show significant underprediction in the near field, but good agreement downstream of about x/D = 20. This suggests that the near field discrepancy in laterally averaged effectiveness shown in Figure 5 is primarily due to initially too slow lateral spreading of the coolant jet after injection. The slow jet more than likely assumes a flat cross section, being squished into the wall when it interacts with the faster mainflow. This perhaps point to isotropy of the turbulence modeling approach as a significant shortcoming for near field predictions at low blowing ratios. The higher M case, where I is high, shows consistent results with Figure 5 above. Specifically, the computations show a rapid rise in effectiveness such that a maximum is reached by about x/D = 30, while the experiments show much slower transport of the coolant back to the downstream surface.

Figure 7 shows the laterally-averaged adiabatic wall effectiveness values for the higher strength-of-curvature case (2r/D = 61). The plot indicates a range of blowing ratios from approximately 1 to 2. Note that the maximum dimensionless downstream distance, x/D, is smaller for these cases, since the same passage test section was used with a larger film-hole diameter. However, the plot abscissa is extended to x/D = 100, to allow easier visual comparison with Figures 5 and 6. Similarities between Figures 5 and 7 are apparent. As above, the computations show an underprediction of the experiments for the lowest M case, with the discrepancy more severe in the near-field region (x/D < 20) than further downstream. However, the middle case, M=1.33, shows the best agreement between CFD and experiments. Not coincidently, it is this blowing ratio that yields a momentum flux ratio closest to unity for all of the cases over both curvatures. As discussed in the literature review, the effect of curvature on the mean flow due to cross-stream pressure gradients is in general a function of the momentum flux ratio I, so that the curvature effect is effectively neutral for I = 1.

The effects of curvature can be effectively isolated by comparing results at identical blowing rates from two strength of curvature cases. The laterally-averaged adiabatic wall effectiveness is shown in Figure 8 for the lowest blowing ratio simulated for each curvature, M = 1. For this blowing rate, the momentum-flux ratio is 0.5. As discussed above, convex curvature influences the mean flow by pushing the jet towards the surface for I < 1, thus increasing the effectiveness over the expected flat-plate value. The plots indicate that this is indeed the case, with increased curvature resulting in higher effectiveness levels, for both computations and experiments. For a given wall curvature, a larger diameter jet comes out of the film hole for the higher strength. A larger jet, at a given blowing rate, has more of its mass away from the wall, traveling a larger radius of curvature. Thus this fluid has a lower centrifugal force, traveling a larger radius of curvature. Hence this portion of the jet, which is farthest from the wall, works to keep the portion of jet below it on the surface. The fact that both experiments and computations respond in a similar manner suggests that the CFD is in fact resolving the

physical mechanisms responsible for the film-cooling performance, at least in a qualitative sense. There are, however obvious differences. The computations show much less of a response to the curvature than the experiments, indicating that the impact of curvature is not fully resolved. This is likely due to the fact that the governing equations are able to capture the mean flow response, but the turbulence model is not able to capture the influence of convex curvature on the turbulent dynamics, including suppression of turbulence and therefore decreased mixing.

Figure 9 shows a comparison of laterally-averaged effectiveness for the two curvatures, at higher blowing rates. For the higher curvature, M = 1.9 is shown, and for the lower curvature two cases are shown, M=1.6 and M=2.5, that bracket M=1.9. There is little difference between the two low curvature results, and so it may be inferred that they are both representative of results at M = 1.9, and can be compared to the higher curvature case. The experiments indicate the expected trend, namely, that an increase in curvature results in decrease in effectiveness for a momentum-flux ratio greater than unity. However, the computations not only indicate an overprediction of effectiveness for all cases, they also do not show the expected decrease in effectiveness that should arise from an increase in curvature. It is likely that the current modeling treatment leads to serious deficiencies when the coolant jets lift-off and penetrate through the boundary layer and into freestream. Further discussion is found in later sections.

4.2 Concave curvature

This section compares the present computational results with the experimental data from Schwarz [8] on the surface with concave curvature. In order to clearly show the effect of curvature, only the CFD simulations for the high strength curvature case are demonstrated. Figure 10 shows the laterally-averaged adiabatic wall effectiveness plotted versus x/D for blowing ratios (M) ranging from 0.9 to 2.2. These plots are obtained by integrating the local lateral profiles of impermeable wall effectiveness using the trapezoidal rule. On the concave surface only one phenomenon – increase in the normal momentum of the jet - degrades the performance. The centrifugal force of the jet, which was detrimental to cooling on the convex surface, enhances performance on the concave surface. For low M, near the injection hole, the normal momentum is less when compared to high M. Hence experiments predict very high performance near injection, but gradually decrease further downstream. Near injection, CFD underpredicts the effectiveness values up to x/D=15 and overpredicts from then on. With increase in x/D, CFD shows better cooling performance, although experiments show low cooling. This is attributed to the fact that on a concave surface, turbulence is enhanced, which in turn improves mixing. The current turbulence model does not incorporate turbulence effects caused by curvature. Hence the model cannot predict the excessive turbulence produced by the concave surface. As blowing rate is increased, the two phenomena mentioned above exert more influence. Near the film hole exit, the normal momentum is dominant and experiments predict that the jets leave the surface immediately after injection. CFD predicts that the jets reattach thermally at a higher x/D than experiments. This discrepancy could be caused by the inability of CFD to correctly predict the jet in crossflow interaction in the presence of concave curvature.

Between x/D = 15 and x/D = 25, the CFD results agree more closely with experiments. In this region, the component of normal momentum becomes small and as the jet takes a curvilinear path, centrifugal forces become dominant. Centrifugal forces are functions of mean flow mechanisms and hence are well predicted by CFD. Figure 10 also shows that with M, the quantitative rise of performance values further downstream (x/D > 25) for both the experiments and the CFD is same. This suggests that CFD is indeed capable of capturing quantitative results in the far field.

5. CONVEX VS. CONCAVE

5.1 Impermeable wall effectiveness

Figure 11 shows the comparison of laterally averaged effectiveness plots for blowing rate close to unity on both the convex and concave surfaces. Note that at this blowing rate, where the centrifugal force is not a dominating factor, the cross-stream pressure gradient tends to push the jets into the convex wall and pull them away from the concave wall. Hence film cooling on convex surface should perform better than the concave counterpart. This case highlights the mean-flow mechanisms of the flow. Clearly CFD predicted better performance on the convex than the concave surface. This agreement might be due to the ability of CFD to predict mean flow mechanisms as discussed above. But there are obvious differences. Farther downstream, CFD overpredicts in the case of concave surface, whereas it underpredicts in the case of convex surface. This could be reasoned as follows. On a convex surface, turbulence is suppressed which results in less mixing with the hot crossflow and results in better cooling performance. The turbulence model used is not capable of responding to such a behavior of the convex surface and hence predicts lower performance in the far field. On a concave surface, turbulence is enhanced which results in greater mixing with the hot crossflow resulting in low performance. Again this is not predicted in the current simulations. In essence, it is the lack of sensitivity of the turbulence field to the curvature effects that is responsible for the discrepancy in this figure.

Figure 13 shows comparison of laterally-averaged profiles for the highest blowing rate close to 2. It is clear that the present modeling technique is unable to accurately predict the performance in these cases. Here, the jets lift-off and go through the boundary layer. The fact that most models are calibrated for boundary layer turbulence leads to severe discrepancies in these cases. This phenomenon is further dealt with in later sections. Both the convex and concave CFD jets predict similar performance indicating no response to the curvature. The comparison of the profiles (Figure 12) of the blowing rate case when I is close to unity show a distinct behavior of the CFD simulations. The mean flow effects on curvature become neutral in these cases. The simulations on the convex curvature agreed well with experiments, but on the concave curvature the computational results departed from experiments. It should be noted that even when I is close to unity, the curvature effects on turbulence dynamics should still be present. Hence it is of no surprise that the computations departed from experiments on the concave curvature film cooling.

5.2 Discussion of Physics

This section focuses on the influence of convex and concave curvature on film-cooling performance, and the ability of commonly used eddy-viscosity based two-equation turbulence models to predict this influence. Those mechanisms unrelated to streamline curvature, yet significant to film-cooling performance, also deserve some attention. This section is divided into two parts: a discussion of the mean-flow physics, as predicted by the CFD simulations, and a discussion of the predicted turbulent mixing effects. The two are strongly coupled in many cases, and as much as possible, the links between them are investigated.

5.2.1 Mean-Flow Physics Mechanisms

In a qualitative sense, the film-cooling flow field on a curved surface is similar to that on a flat plate. Many of the same physical mechanisms are apparent in both cases. The present results share many of the features discussed in Walters and Leylek [17].

The current results show the presence of a horseshoe vortex upstream of the film-hole exit, illustrated in Figure 14. Here the formation of vortex on convex side is demonstrated. The horseshoe vortex forms due to the roll up of vorticity contained in the approaching crossflow boundary layer. The figure indicates the expected trend that the strength of the vortex is greatest for low coolant injection rates, and is reduced as blowing rate increases. It is shown in earlier studies that the horseshoe vortex may play a role in determining the film-cooling performance in the near field, since it may entrain coolant fluid and transport it upstream and to the sides of the film hole on the cooled surface. In a thesis recently presented by Rawlings [24] demonstrated the formation of a round horseshoe vortex using the unsteady RANS approach. The author also performed the simulations using the RKE model used in the present study and showed a flattened shape of the horseshoe vortex, similar to Figure 14. However, Rawlings [24] observed this in a normal jet in crossflow problem, although similar mechanisms are thought to act in the present inclined-jet cases. It is also known that the impact of the horseshoe vortex on film cooling is sensitive to developing boundary layer. Since convex curvature impacts the developing boundary layer (Muck et al., [3]), and the current turbulence model does not respond to streamline curvature, it is likely that the boundary-layer history is not properly predicted, and therefore the influence of the horseshoe vortex not quantitatively resolved in the present CFD simulations. This may explain, in part, the lack of lateral coolant spreading in the near field, as shown in Figure 6. Rawlings [24] very clearly demonstrated the lack of spreading in his RKE simulations when compared with the unsteady RANS approach. A horse shoe vortex similar to Figure 14 is also indicated by the simulations on the concave surface.

Jet lift-off plays a very important role in the cooling effectiveness as well as in the ability of the computations to reproduce the experimental results. This jet lift-off mechanism is closely related to the presence of a counter-rotating vortex (CRV) pair downstream of coolant injection, one of the prominent features discussed in film-cooling studies. As discussed in Walters and Leylek [17], the primary source of vorticity in the near field is that contained in the film-hole boundary layers exiting the film hole. CRVs are responsible for the entrainment of the hot crossflow beneath the jet at higher blowing rates. Some amount of vorticity is also generated at the jet-crossflow interface, due to pressure gradients acting normal to the coolant-freestream density gradients. One significant effect of curvature is to redirect the normal component of vorticity to the wall so that it is oriented in the direction of flow. Likewise it redirects vorticity oriented in the flow direction so that it is oriented normal to wall. Due to this action, the CRVs may be strengthened or weakened. For flow over convex surfaces, the coolant is effectively pushed toward the surface for momentum flux ratios less than unity. For $I > 1$, on the other hand, the coolant is lifted away from the surface due to centrifugal forces, and correspondingly the CRVs are strengthened by the effects of curvature. The opposite action occurs for film cooling on concave surfaces. Figure 15 illustrates the CRV secondary flow superimposed on the contours of coolant species mass fraction at two locations ($x/D = 2$ and 10) and two blowing rates ($M = 1$ and 2.5) for the low convex curvature case ($2r/D = 126$). It is apparent that immediately downstream of the film hole ($x/D = 2$) both blowing rates indicate the presence of counter rotating vortices and a corresponding impact on the distribution of the exiting coolant. However, farther downstream, at $x/D = 10$ only the highest M case still clearly shows the presence of secondary motion. The CRVs persist father downstream in this case due primarily to the effects of curvature. The simulations on the concave side also predicted secondary motions and indicated the expected trend. At high blowing rate, the coolant strikes the curved concave surface resulting in attenuation of CRVs. The counter rotating vortices persist in the case of the low-momentum coolant on the concave curvature. However, computations tend to overpredict this secondary flow because of the lack of the ability of RKE model to resolve the impact of curvature on turbulence field.

5.2.2 Turbulent Mixing

The effectiveness results presented for convex curvature cases in section 4.1 indicate that the computations underpredict the experiments for low blowing rates, and overpredict the experiments for higher blowing rates. Further, the degree of discrepancy is greater for higher blowing rates. Also the figures in section 4.2 and 5.1 suggest that the computations perform most favorably for cases when the coolant remains within the boundary layer, and does not lift-off from the downstream surface. It may be reasoned that there is a fundamental shortcoming to this modeling approach for cases involving significant jet lift-off. This shortcoming is likely traced to the traditionally poor performance of steady RANS models for flows with significant flow separation. This has been supported by the recent research conducted by Rawlings [24]. This shows that the CFD can not predict accurately the lift-off mechanism.

One of the reasons for disappointing performance of the simulations for lifted-off cases may be related to the fact that all RANS models are calibrated to yield results in turbulent flows that are near or at equilibrium. These flows include the inertial layer in the turbulent boundary layer, decaying freestream turbulence, and far-field regions of free jets and wakes. In film cooling flows with high lift off, where there is massive separation in the near-field region of jets, the turbulence structure may be said to be more closely resembling an unsteady periodic with the energy concentrated at or near one or more characteristic frequencies (Yule [25]). The dynamics is very closely linked to the problem geometry. This type of unsteady behavior has been documented experimentally in the near field region of film-cooling flows (Kohli and Bogard [26]). It is possible that real improvement in the predictive capability of CFD for high M will necessarily require a methodology that moves beyond typical steady Reynolds-averaged simulations, and include the resolution of the unsteady flow field in the vicinity of the jet exit. Therefore one major conclusion of this study is that the steady, RANS-based modeling approaches as they currently exist are unlikely to yield consistently accurate results for film cooling with highly detached coolant jets, regardless of streamline curvature, freestream turbulence, and/or streamwise pressure gradient effects.

Another well known limitation of the current turbulence treatment is the lack of anisotropy in the eddy-viscosity approach. Both the Reynolds stress tensor and the turbulent heat flux are based on simple gradient-based approximations, with a single scalar turbulent viscosity (diffusivity). The effect of this shortcoming is apparent in the lack of coolant spreading in the lateral direction, shown by the computational results in Figure 6. The lack of lateral coolant spreading in the lateral direction can also be seen in Figure 16, which shows the contours of adiabatic wall effectiveness on the downstream surface, for the bounding blowing ratios examined on the convex curvature (high strength) and concave curvature. It is possible that the effect of unsteady, non-equilibrium turbulence

discussed is closely related to turbulence anisotropy. A methodology that resolves near field unsteadiness would improve the ability to resolve lateral coolant spreading.

The impact of streamline curvature on the turbulent mixing – and the subsequent impact on cooling effectiveness -- remains to be discussed. The primary goal of the present study was to isolate the ability of RKE, representative of two-equation eddy viscosity family of turbulence models, to capture the response of curvature by minimizing all other sources of error. While it is believed that this has been done, it is difficult to quantify what weaknesses in the current turbulence treatment are due to curvature effects and what weaknesses are due to other effects discussed above (unsteadiness, anisotropy, etc.). It appears that curvature effects are only secondary at high blowing rates. However, low M cases, in which the coolant remains attached within the boundary layer, show reasonable agreement with experiments, and it is these cases that highlight the effects of curvature on the turbulent mixing process. Consider Figure 8, which shows laterally-averaged effectiveness versus downstream distance at equivalent (low) blowing ratios, and two different rates of convex curvature. It is expected that an increase in convex curvature will suppress turbulence in the boundary layer and therefore turbulent mixing of the coolant. This should result in an increased value of downstream effectiveness, assuming other governing parameters remain unchanged. This effect is dramatically visible in the experimental data. The computations, however, show only a slight response to the increased curvature effects. It is likely that the computations are resolving only the curvature effect on mean-flow physics, and so underpredict the curvature response. In contrast, Figure 9 shows that both computations and experiments show much less response to an increase in curvature for cases when the coolant jet is lifted far from the downstream surface. The significant difference between the CFD and experimental results must be due to other mechanisms, as discussed above.

SUMMARY AND CONCLUSIONS

This study documents the computational simulation of film-cooling flow over convex and concave surfaces. The general objective is to assess the ability of CFD to capture curvature effects in many complex situations such as fan aero, compressor aero, turbine aero and heat transfer applications. The study utilized a systematic computational methodology to minimize errors due to computational model, grid, and discretization scheme, and to place the results firmly against the limits of the turbulence modeling technique. The specific turbulence model used in the present study was representative of currently popular two-equation modeling practice, and was accomplished using the realizable k-ε model (RKE) of Shih et al. [21], and two-layer near-wall treatment of Wolfstein [22]. Examination of the results yield the following conclusions:

- The simulations demonstrated an ability to resolve laterally averaged film-cooling performance with reasonable accuracy for cases with low blowing ratios (i.e. cases in which the coolant jet did not lift-off from the downstream surface, but remained within the boundary layer).
- For cases with relatively high blowing ratios, the coolant lifted off from the downstream surface, and the computations were unable to accurately resolve the cooling effectiveness.
- The computations indicated the correct qualitative response of downstream cooling performance to curvature, particularly at low M. However, there are obvious discrepancies due to the lack of response by the RKE turbulence model to streamline curvature effects. Future improvements to predictive capability will likely require either the use of more advanced models (differential or algebraic Reynolds stress models) or the modification of eddy-viscosity models to include the effects of curvature.
- For cases with high blowing ratios, the influence of curvature appeared to be secondary to other likely sources of discrepancy. Specifically, these include unsteady (non-equilibrium) influences in the near-field region associated with jet lift off, and turbulence anisotropy. Future modeling improvements for simulation of highly lifted-off coolant jets will likely require some method of including these effects, either through improved steady modeling capability or through the use of time-resolved (unsteady) modeling approaches, or both.
- Overall, the present study indicates that current modeling practice is adequate to predict film-cooling performance on curved surfaces provided that the blowing ratio is low enough that the coolant jet is not lifted far from the surface. The Computations failed when the major influence of curvature is on the Reynolds stresses and turbulent heat fluxes. Future improvements to modeling technology, as suggested above, will increase the general level of applicability of CFD to film-cooling problems.

ACKNOWLEDGEMENTS

This research was sponsored by the U.S. DOD. The authors are grateful for the support.

REFERENCES

[1] Bradshaw P.,1973, “Effects of streamline curvature on turbulent flow”, AGARDograph, 169.

[2] So, R.M.C. and Mellor, G. L.,1973 “Experiments on convex curvature Effects in turbulent boundary layers,” Journal of Fluid Mechanics, 60, no.1, pp 43-62.

[3] K. C. Muck, P. H. Hoffmann and P. Bradshaw, 1985, “The effects of convex surface curvature on turbulent boundary layers,” Journal of Fluid Mechanics, 161, pp 347-369.

[4] K. C. Muck, P. H. Hoffmann and P. Bradshaw, 1985, “The effects of concave curvature on turbulent boundary layer,” Journal of Fluid Mechanics, 161, pp 371-403.

[5] S. Ito, R. J. Goldstein, E. R. G. Eckert, 1978, “Film cooling of a gas turbine blade,” Journal of Engineering for power, 100, pp 476-481.

[6] R. J. Goldstein, Y. Kornblum, E. R. G. Eckert, 1982, “Film Cooling Effectiveness on a Turbine Blade”, Israel Journal of Technology, 20, pp. 193-200.

[7] M. Makino, M. Kumada, 1987a, “Effects of wall curvature on the full-coverage film cooling effectiveness”, Heat Transfer and fluid flow in rotating machinery, W.J Yang(ed), pp. 103-112.

[8] Schwarz, S. G., 1986, “Film cooling of curved surfaces,” Ph.D. Thesis, University of Minnesota, MN.

[9] Schwarz, S.G. and Goldstein, R.J.,1988, "The Two-Dimensional Behavior of Film-Cooling Jets on Concave Surfaces," ASME Journal of Turbomachinery, 111, pp. 124-130.

[10] S. G. Schwarz, R. J. Goldstein, E. R. G. Eckert, 1991, "The influence of curvature on film cooling performance," Journal of Turbomachinery, 113, pp. 27-33.

[11] E. Lutum, J. von Wolfersdorf, B. Weigand, K.Semmler, 2000, "Film cooling on a convex surface with zero pressure gradient flow," International Journal of Heat and Mass Transfer, 43, pp. 2973-2987.

[12] Walters, D. K. and Leylek, J. H., 1997, "A Systematic Computational Methodology Applied to a Three-Dimensional Film-Cooling Flowfield," ASME Journal of Turbomachinery, 119, pp. 777-785.

[13] Berhe, M. K., and Patankar, S. V., 1999a, "Curvature effects on discrete-hole film cooling," ASME Journal of Turbomachinery, 121, pp.781-791.

[14] Berhe, M. K. and Patankar, S. V., 1999b, "Investigation of Discrete-Hole Film-Cooling Parameters Using Curved-Plate Models," ASME Journal of Turbomachinery, 121, pp. 792-803.

[15] Y. L. Lin and T.I-P Shih, "Computations of discrete-hole film cooling over flat and convex surfaces," ASME paper no. 98-GT-436.

[16] R. E. Mayle, F. C. Kopper, M. F. Blair, D. A. Bailey, 1977, "Effect of streamline curvature on film cooling," Journal of Engineering for power, 99, pp 77-82.

[17] Walters, D.K. and Leylek. J.H., 2000a, "A Detailed Analysis of Film-Cooling Physics -- Part1: Streamwise Injection with Cylindrical Holes," ASME Journal of Turbomachinery, 122, pp. 102-112.

[18] Durbin, P.A., 1996, "On the k-ε Stagnation Point Anomaly," International Journal of Heat and Fluid Flow, 17, pp. 89-90.

[19] Joan G. Moore and John Moore, 1999 "Realizability in Turbulence Modeling for Turbomachinery CFD," ASME paper no. 99-GT-24.

[20] Walters, D.K. and Leylek. J.H., 2000b, "Impact of Film-Cooling Jets on Turbine Aerodynamic Losses," ASME Journal of Turbomachinery, 122, pp.537-545.

[21] Shih, T. –H., Liou, W. W., Shabbir, A., and Zhu, J., 1995, "A New k-ε Eddy-Viscosity Model for High Reynolds Number Turbulent Flows: Model Development and Validation," Computers and Fluids, 24, pp. 227-238.

[22] Wolfstein, M., 1969, "The Velocity and Temperature Distribution of One-Dimensional Flow with Turbulence Augmentation and Pressure Gradient," International Journal of Heat and Mass Transfer,12, pp. 301-318.

[23] Chen, H.C. and Patel, V.C., 1988, "Near-Wall Turbulence Models for Complex Flows Including Separation," AIAA Journal, 26, pp. 641-648.

[24] Christopher K. Rawlings, 2002, "Physics Based Prediction of Low Velocity Ratio Jet/Crossflow Interaction In Computational Film Coolin Simulations," Master's Thesis, Clemson University, SC.

[25] Yule, A.J., 1978, "Large-Scale Structure in the Mixing Layer of a Round Jet," Journal of Fluid Mechanics, 89, pp. 413-432.

[26] Kohli, A. and Bogard, D.G., 1998, "Effects of Very High Free-Stream Turbulence on the Jet-Mainstream Interaction in a Film-Cooling Flow," ASME Journal of Turbomachinery, 120, pp. 785-790.

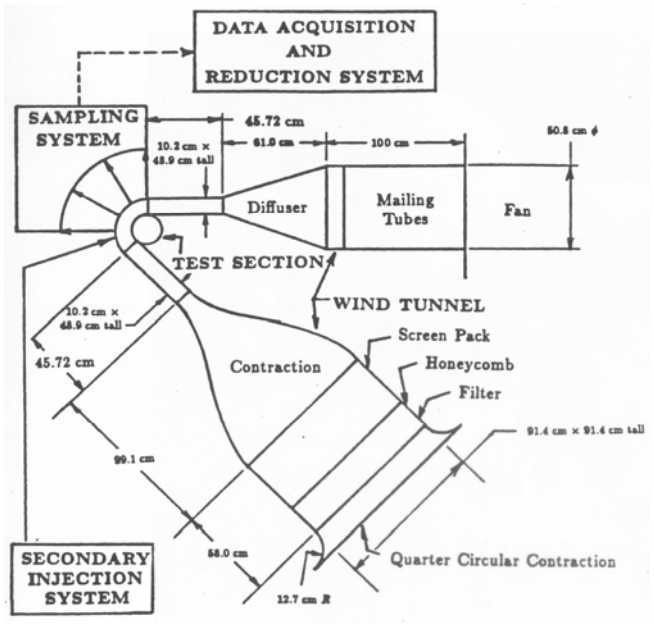

Figure 1. Illustration of the apparatus used in the experimental test cases (Schwarz [9]).

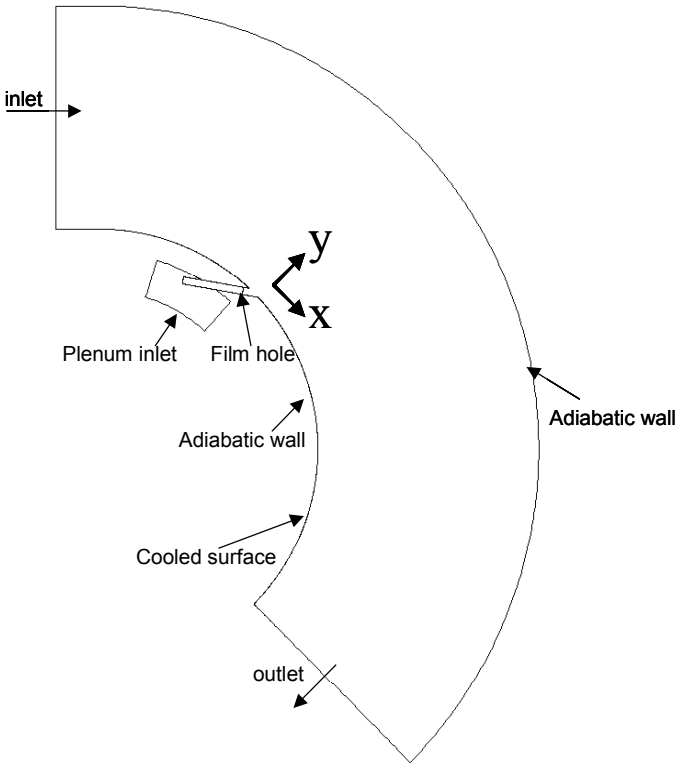

Figure 2. Illustration of the computational domain used in the convex curvature film cooling study.

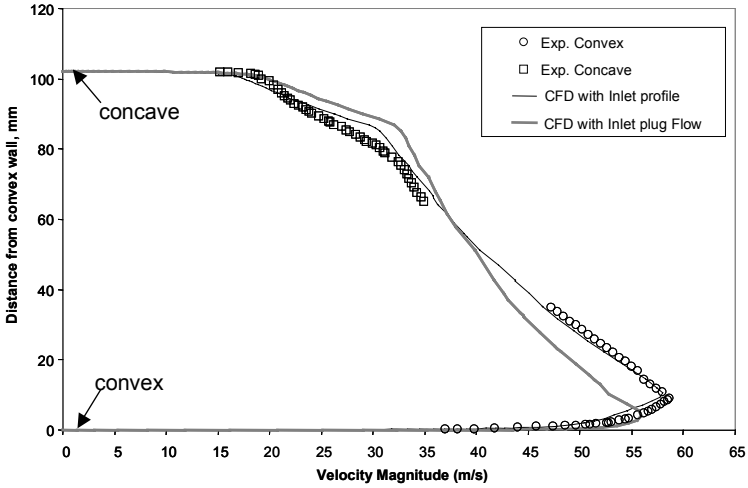

Figure 3. Velocity profile at the jet injection location for the convex surface. Comparison is shown between experimental data, present inlet profile, and plug-flow inlet.

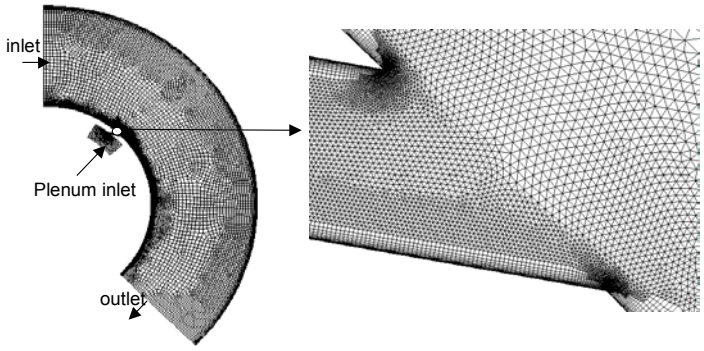

Figure 4 (a). Centerplane background mesh used in the convex curvature film cooling study, including close-up of the film-hole exit region.

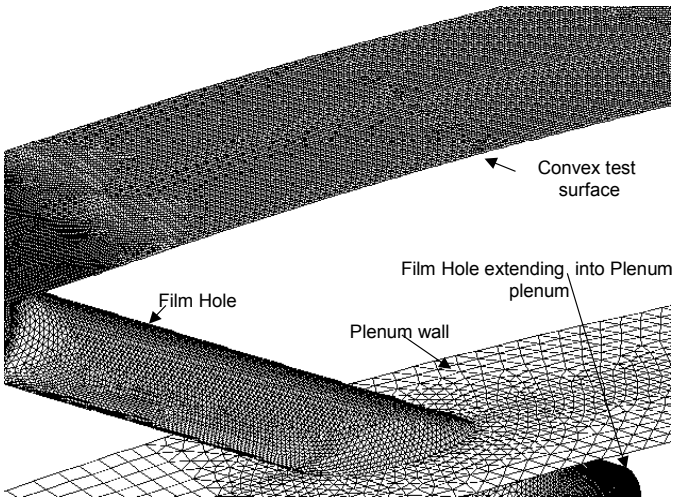

Figure 4 (b). Surface mesh showing the film-hole inlet and supply plenum region.

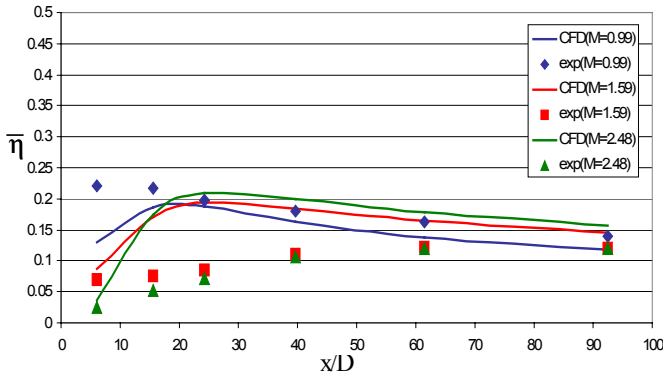

Figure 5. Laterally-averaged adiabatic wall effectiveness versus downstream distance for the low strength convex curvature case (2r/D = 126), DR = 2.

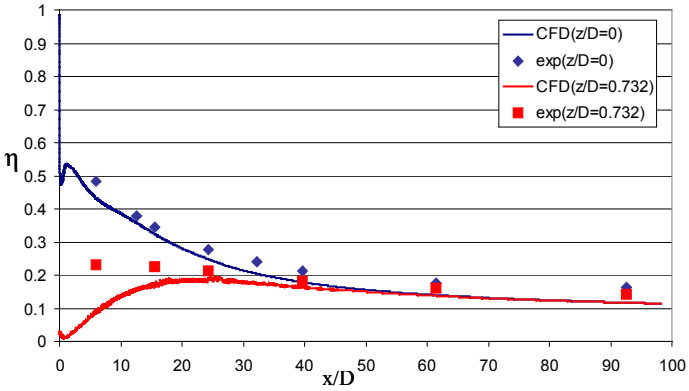

a) M = 1.00, DR = 2.

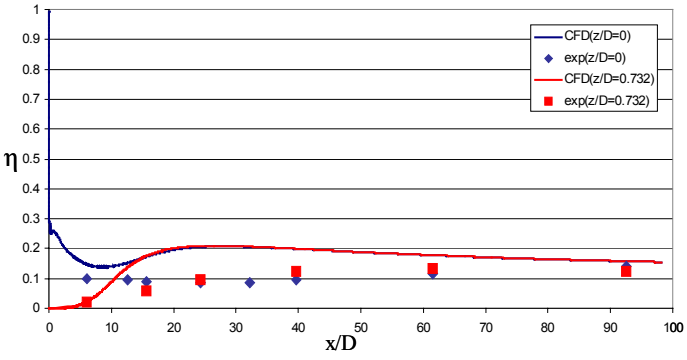

b) M = 2.5, DR = 2.

Figure 6. Local variation of impermeable wall effectiveness versus downstream distance at two different spanwise locations. Low strength convex curvature case (2r/D = 126); M = 1 (a) and M = 2.5 (b).

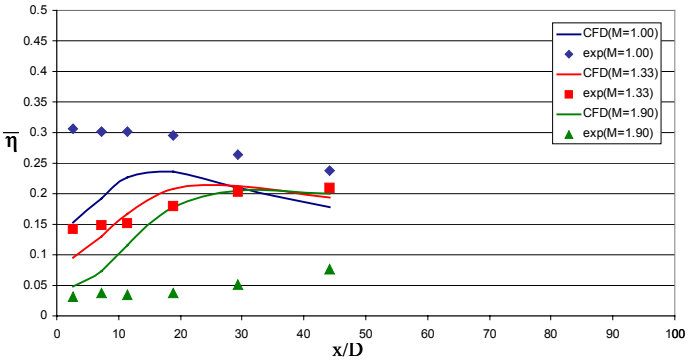

Figure 7. Laterally-averaged adiabatic wall effectiveness for high strength convex curvature case (2r/D = 61), DR = 2.

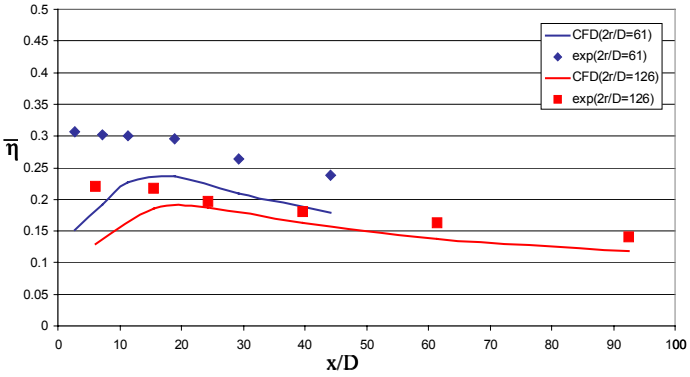

Figure 8. Comparison of laterally-averaged effectiveness for two strength of convex curvature cases, M = 1, DR = 2.

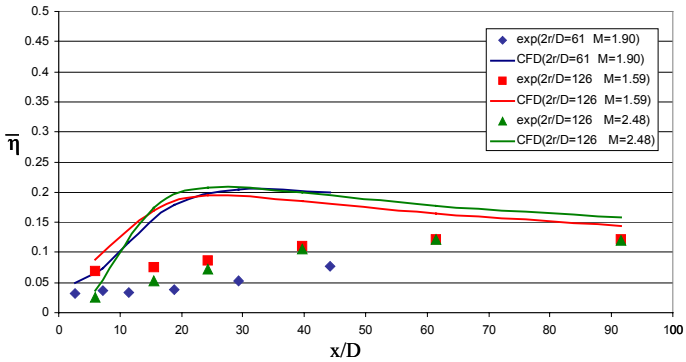

Figure 9. Comparison of laterally-averaged effectiveness for two strength of convex curvature cases, at high blowing ratios, DR = 2.

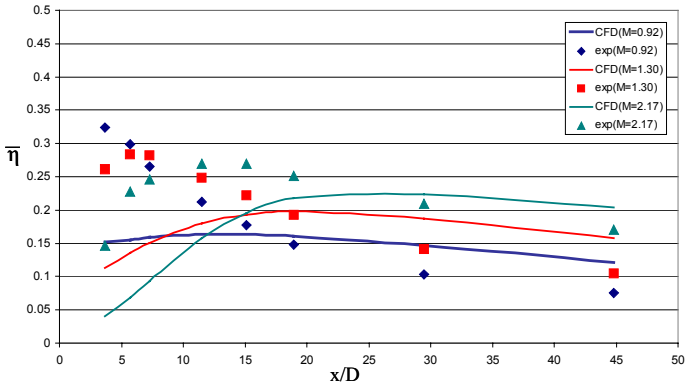

Figure 10. Streamwise variation of laterally-averaged adiabatic wall effectiveness for the concave curvature (2r/D = -58), DR = 2.

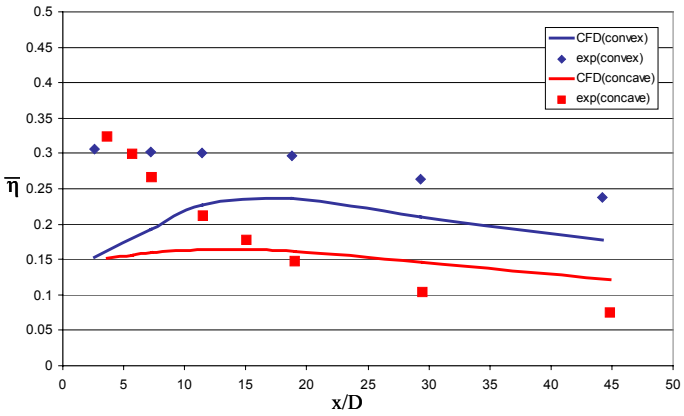

Figure 11. Comparison of laterally-averaged wall effectiveness for convex (2r/D = 61) and concave curvature (2r/D = -58) for M = 1, DR = 2.

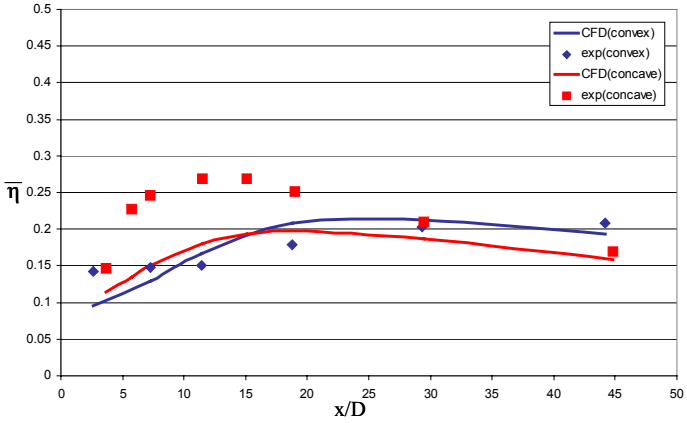

Figure 12. Comparison of Laterally-averaged wall effectiveness for convex (2r/D = 61) and concave curvature (2r/D = -58) for M = 1.30, DR = 2.

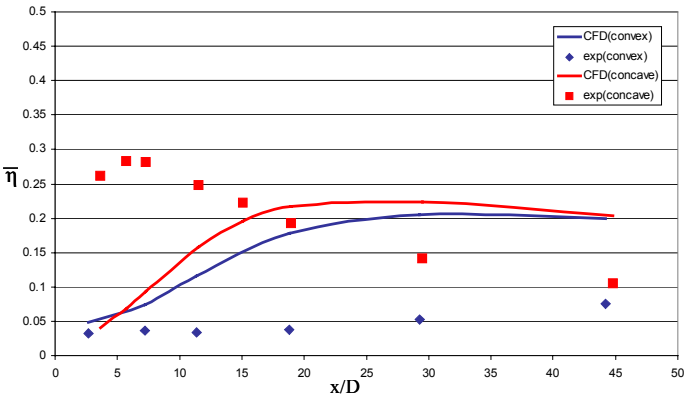

Figure 13. Comparison of Laterally-averaged wall effectiveness for convex (2r/D = 61) and concave curvature (2r/D = -58) for M = 2, DR = 2.

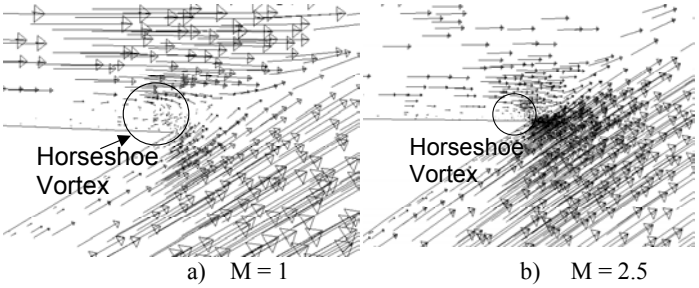

Figure 14. Velocity vectors showing horseshoe vortex formation upstream of the exiting coolant for the low strength convex curvature case. The horseshoe vortex is more pronounced for M = 1 (a) than for M = 2.5 (b), DR = 2.

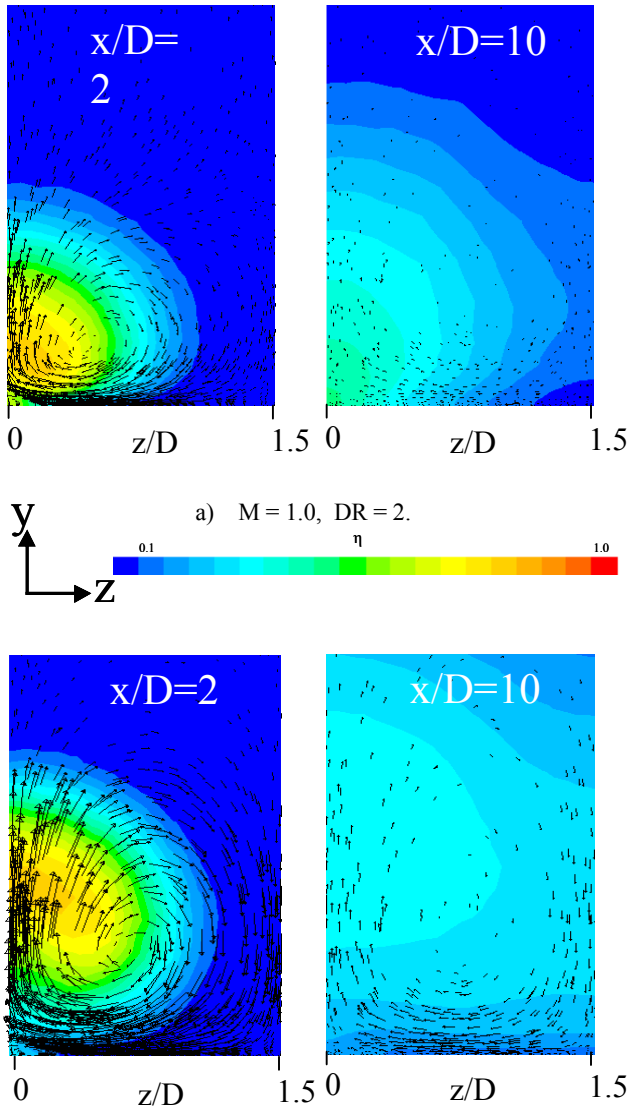

a) M = 1.0, DR = 2.

b) M = 2.5, DR = 2.

Figure 15. Contours of coolant mass fraction superimposed with velocity vectors in planes normal to the local streamwise direction at two downstream locations on convex surface (2r/D = 126). Cases shown are for M = 1 (a) and M = 2.5 (b).

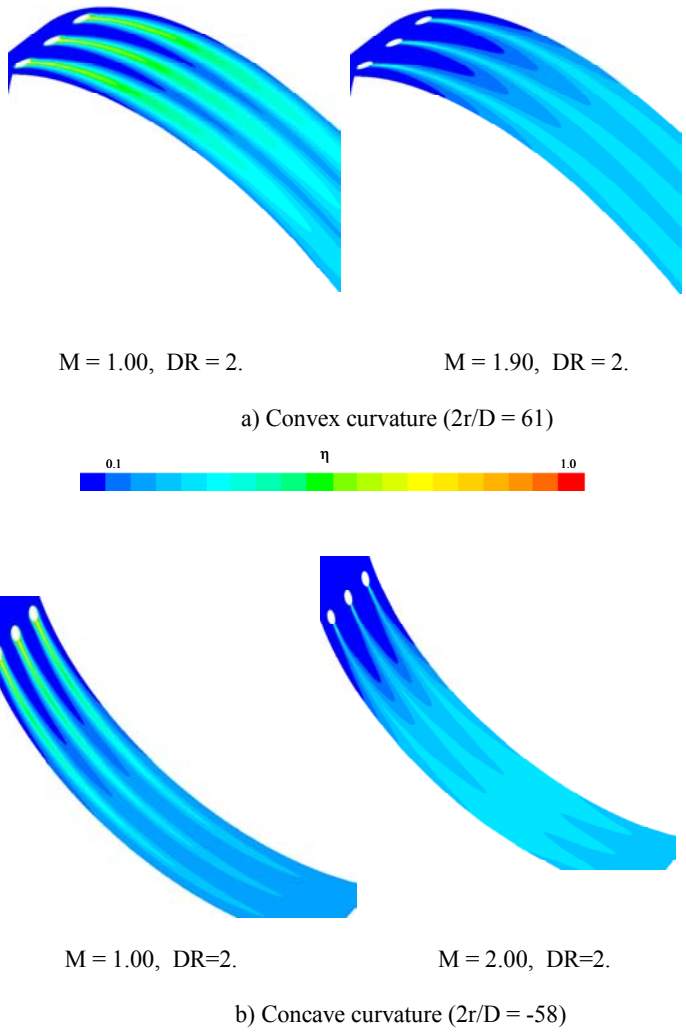

M = 1.00, DR = 2. M = 1.90, DR = 2.

a) Convex curvature (2r/D = 61)

M = 1.00, DR=2. M = 2.00, DR=2.

b) Concave curvature (2r/D = -58)

Figure 16. Contours of impermeable wall effectiveness for the bounding blowing ratios.